Propagation of the Ignition Front in Beds of Wood Particles

J. J. SAASTAMOINEN* and R. TAIPALE
VTT Energy, P.O. Box 1603, FIN-40101 Jyväskylä, Finland

M. HORTTANAINEN and P. SARKOMAA
Lappeenranta University of Technology, Department of Energy Technology, P.O. Box 20, FIN-53851, Lappeenranta, Finland

The speed of the propagation of the ignition front downwards against the air flow in a fixed bed of burning wooden particles has been studied. The ignition speed reaches a steady state soon after ignition at the surface, if the inlet air temperature is the same as the initial temperature of the fixed bed. Modeling of the quasi-steady-state speed of propagation of the ignition front is considered. The effects of the flow rate of air, moisture, particle size, density, and wood species on the velocity of the ignition front and on the maximum temperature in the bed are studied experimentally and interpreted by modeling. A maximum speed of propagation was observed with a specific air rate. Correlations for estimating the velocity of the ignition front and maximum temperature in the bed are presented.

NOMENCLATURE

a	thermal diffusivity, $a = \lambda/(\rho c)$, $m^2\ s^{-1}$
c	specific heat, $J\ kg^{-1}\ K^{-1}$
$\dot{C}''$	flux of heat capacity, $\dot{C}'' = c\dot{m}''$, $W\ m^{-2}\ K^{-1}$
C'''	heat capacity per unit volume, $(1 - \epsilon)\rho_p c_p$, $J\ m^{-3}\ K^{-1}$
d	particle diameter, m
ΔH	effective heat of combustion, $J\ kg^{-1}$
h	heat transfer coefficient, $W\ m^{-2}\ K^{-1}$
K	effective radiation coefficient
l	heat of vaporization or pyrolysis, $J\ kg^{-1}$
M	molecular weight, kg/kmol
$\dot{m}''$	mass flux, $kg\ m^{-2}\ s^{-1}$
Q'''	energy/volume, $J\ m^{-3}$
q''	heat flux, at ignition front $q''_0 = KT_f^4$, $W\ m^{-2}$
q'''	rate of heat generation per unit volume, $W\ m^{-3}$
R	thickness of a plate, radius of a cylinder or a sphere, m
r	coordinate inside a particle, m
S'''	surface area of particles per unit volume of bed, $S''' = (1 + \Gamma)(1 - \epsilon)/R$, m^{-1}
T	temperature, K
t	time, s
U	dimensionless ignition velocity, $U = C'''w_{ig}/\dot{C}''_g$
U_*	dimensionless ignition velocity, $U_* = R^2\alpha w/a_p$
u	moisture content (dry basis), mass of water per unit mass of dry solid
v	mass fraction of volatile matter in dry ash-free fuel
w	velocity, $m\ s^{-1}$
x	coordinate, m
x_*	moving coordinate, m
Y_{O2}	mass fraction of oxygen in gas (0.232 for air)

Greek Symbols

α	decay coefficient, m^{-1}
Γ	particle shape factor, 0 for a plate, 1 for a cylinder, 2 for a sphere
δ	thickness, m
ϵ	porosity of bed
η	coefficient for heat recovery to gas flow
ϑ	dimensionless gas temperature, $\vartheta = (T_g - T_\infty)/(T_{ig} - T_\infty)$
θ	dimensionless particle temperature, $\theta = (T_p - T_\infty)/(T_{ig} - T_\infty)$
Λ	dimensionless parameter, $\Lambda = hS'''/(\alpha\dot{C}''_g)$
λ	thermal conductivity of dry layer, $W\ m^{-1}\ K^{-1}$
κ	coefficient for char temperature at reaction zone

*Corresponding author. E-mail: Jaakko.Saastamoinen@vtt.fi

0010-2180/00/$–see front matter
PII S0010-2180(00)01144-9

COMBUSTION AND FLAME 123:214–226 (2000)

Published by Elsevier Science Inc.

ξ dimensionless coordinate, $\xi = hS'''x_*/\dot{C}''_g$
ρ density, mass/volume, kg m^{-3}
σ Stefan-Boltzmann's constant, $5.67 \cdot 10^{-8}$ W m^{-2} K^{-4}
Φ dimensionless heat flux, $\Phi = \alpha q''_0 R/[S'''\lambda_p(T_{ig} - T_\infty)] = \alpha q''_0 R^2/[(1 + \Gamma)(1 - \epsilon)\lambda_p(T_{ig} - T_\infty)]$
ϕ dimensionless ignition parameter, $\phi = (q'''/hS''')/(T_{ig} - T_\infty)$

Subscripts

0 at ignition front
∞ initial, inlet, far from ignition front
a adiabatic
b dry bed
c char
f effective flame seen from the ignition plane
g gas
ig ignition
max maximum
p dry particle
vap vaporization, water vapor
vol devolatilization, volatiles
w liquid water

INTRODUCTION

There is a vast literature on both experiments and models of the propagation of forest and grass fires [1–8], but their applicability to combustion in fuel beds used for energy production is limited. In furnaces the fuel beds are much denser. The speed of the ignition front with combustion on a grate is of practical interest. Ignition in the combustion of coal [9–13] or wastes [14–18] on a grate has been studied and also summarized [19]. Recently, there has been new interest in combustion or gasification [20, 21] on a grate, as used for generating small and medium-scale heat and power. Wood and biomass combustion is feasible only in small and medium-scale furnaces, since wood must not be transported too far due to high costs. Some models for the propagation of combustion in fixed beds [22, 23] have been presented. Combustion of wood or biomass particles in fixed beds has been studied experimentally [24–30] and by modeling [25, 31]. Experimental results and modeling of the flame speed in a bed of wooden particles are presented in this paper. The ignition front propagates to the initially cool bed against the flow of air. There is an analogy between a fixed bed and a moving bed [32] and the results can be applied to estimate ignition above traveling grates.

The use of wood and biomass as fuels is expected to increase in the future, because of the need to decrease carbon dioxide emissions. In addition, incineration is becoming more important for solid waste, with the beneficial side effect of producing energy. Waste disposal by landfill is expensive and often impossible. Knowledge of the factors affecting the speed of the ignition front is important, since this velocity often determines the heat output from the grate's area. The release of volatiles, volatile nitrogen species (NH_3 and HCN), and NO formed from volatiles is directly related to the speed of the ignition wave inside the bed. Furthermore, knowledge of ignition is important for optimizing gas-phase combustion above the bed to minimize emissions. In this paper, flame propagation in underfed combustors is considered, i.e., the combustion air flows against the propagation of the ignition front. The results can also be applied to traveling grates, where the fuel is ignited on top of the bed and the air flows upwards through the grate and the bed, as depicted in Fig. 1.

EXPERIMENTAL

Two pot furnaces were used: A at VTT Energy (VTT) and B at Lappeenranta University of Technology (LUT). Pot furnace A (diam. 244 mm and height 300 mm) was on a balance. Pot furnace B had a square cross-section (150 mm $\times$ 150 mm $\times$ 900 mm). One fuel (fuel *a*) was used with furnace B and several fuels (*b*, *c*, *d*, *e*) were used with furnace A. Fuel *a* consisted of thin wood chips (mixture of spruce and pine) produced when notches of construction baulks are cut. Thus, the particles were quite long ($\sim$35 mm) and thin (thickness $\sim$1 mm). Average fuel moisture contents were specially prepared to have three different values, namely 8.9, 17.3, and 29.7 wt % (wet basis) for fuel *a*. Likewise, the average measured bulk density of the beds

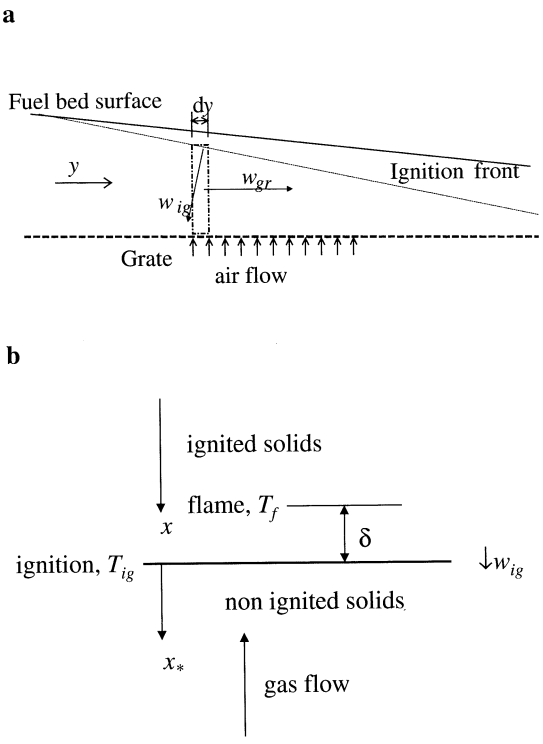

Fig. 1. (a) Analogy between combustion in a fixed bed and on a grate. The box drawn with the dashed line is a control volume which corresponds to a fixed bed. (b) Propagation of an ignition plane in a fixed bed.

(ρ_b calculated for dry fuel) had one of three values: 58.4, 57.5, and 75.7 kg m^{-3}, respectively. The moisture contents of the medium size particles *b* (sieved spruce wood chips, 5–20 mm) were 10.8, 18.8, 27.1, and 33.5% and the corresponding dry bed densities were 157, 145, 142, and 140 kg m^{-3}, respectively. The largest particles *c* (30 mm) were a mixture of spruce and pine, almost dry (2.1% wet basis) and the dry bed density was 230 kg m^{-3}. In addition, two particle sizes of both birch (*d*) and alder (*e*) were studied. The shape of *c* particles was approximately cubic. The shape of the other fuels was typical of wood chips with one dimension smaller than the other two.

An example of temperature measurements inside the fuel bed is presented in Fig. 2. The flame speed inside the fuel bed was calculated by measuring the times needed for temperature waves of 673, 773, and 873 K to travel the distance between two thermocouples. The flame speed was calculated as the average of these values.

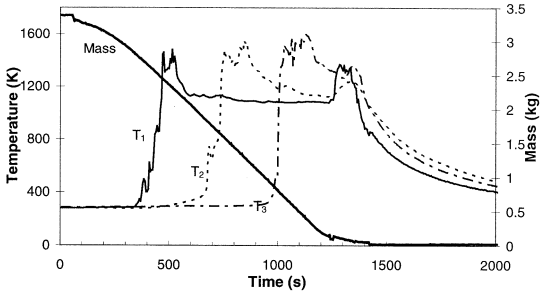

Fig. 2. A pot furnace experiment for the study of the combustion rate of a wood chip layer (fuel *d*). Measured mass of the layer and temperatures inside the fuel bed as function of time. Locations of temperature measurements 1, 2, and 3 are 250, 148, and 50 mm from the bottom of the bed, respectively. The mass flow rate of air was 0.15 kg m^{-2} s^{-1} with sieved (SCAN-CM 40:88 standard) birch chips 13 mm, moisture 12.8% (wet basis).

MODELING

The distance from the fuel's inlet at which the surface of a moving bed is ignited depends on the radiation to the bed and on the density and specific heat of the fuel. In addition, wood contains a significant amount of moisture, which greatly affects the distance traveled before ignition occurs. A simplified formula for estimating the ignition distance of the top surface of the fuel, including the effect of moisture, has been presented [33]. In this case there is an ignition source (a flame) in the moving front and the temperature for ignition is much lower (~630 K) in piloted ignition [34, 35] than for spontaneous ignition [36], where no flame is initially available in the neighborhood.

After ignition at the surface, a flame starts to propagate downwards into the bed against the air flow. Again, there is a flame present and piloted ignition is assumed to take place, when the solid's surface reaches a given ignition temperature, T_{ig}, due to the burning of volatiles from the surface. After some time the ignition wave stabilizes to a constant velocity and the system can be treated as a wave in an infinite medium. This system under study is presented in Fig. 2. The main mechanism causing the ignition front to propagate is assumed to be radiation, since air is in counterflow, but conduction and gas mixing near the flame front are also important. Turbulent mixing and combustion near the flame front, together with radia-

tion, are difficult to model, even for a bed consisting of regular particles. The wooden chips used in commercial boilers are irregular with a size distribution and random orientation. From a practical point of view, simple models with suitable experimental parameters to account for randomness seem more useful than highly sophisticated models. In the models presented here, it is assumed that the local absorption of energy in the bed is directly proportional to the local heat flux. Then the heat flux from the burning particles through the bed decays exponentially with distance, $q'' = q''_0 \exp(-\alpha x_*)$, which gives the local heat generation $q''' = -\mathrm{d}q''/\mathrm{d}x = \alpha q''_0 \exp(-\alpha x_*)$. The relationship $\alpha = S'''/4$ has been presented for randomly arranged fuel elements, provided they have no negative curvature [1]. An alternative approach is to lump the complicated processes in the fuel bed in an overall thermal heat conductivity, λ, where the effect of radiation is included in the dependence $\lambda \sim T^3$. Then the problem is reduced to a simple heat conduction model [16].

Thin Dry Solids Including the Effect of Convection

The particles are so thin that their temperature can be assumed uniform. The heating of the oxidizing gas flowing against the moving ignition wave is described by the energy equation

$$\dot{C}''_g \frac{\partial T_g}{\partial x} = hS'''(T_g - T_p) \tag{1}$$

where the term on the right-hand side describes the convective heat exchange between the gas and particles. The heating of the solid fuel in the bed is described by

$$C''' \frac{\partial T_p}{\partial t} = hS'''(T_g - T_p) + q''' \tag{2}$$

The boundary condition far from the ignition front is $T_p(\infty) = T_g(\infty) = T_\infty$. The location of the moving ignition front is propagating with a steady velocity w_{ig}. We apply a new moving coordinate $x_* = x - w_{ig}t$ and obtain

$$\dot{C}''_g \frac{\mathrm{d}T_g}{\mathrm{d}x_*} = hS'''(T_g - T_p) \tag{3}$$

$$-C'''w_{ig} \frac{\mathrm{d}T_p}{\mathrm{d}x_*} = hS'''(T_g - T_p) + q''' \tag{4}$$

Equations 3 and 4 can be presented in dimensionless form as

$$\frac{\mathrm{d}\vartheta}{\mathrm{d}\xi} = \vartheta - \theta, \quad -U \frac{\mathrm{d}\theta}{\mathrm{d}\xi} = \vartheta - \theta + \phi \tag{5}$$

By eliminating θ, we obtain

$$U\vartheta'' - (1 + U)\vartheta' = \phi \tag{6}$$

Equation 6 can be integrated to yield:

$$\vartheta' - (1 + 1/U)\vartheta = \vartheta'(0) - (1 + 1/U)\vartheta(0) + \phi_0\Lambda[1 - \exp(-\xi/\Lambda)]/U \tag{7}$$

The temperatures of the gas and solid can be derived in the form:

$$\vartheta = \frac{\phi_0\Lambda \exp(-\xi/\Lambda)}{U(1 + 1/\Lambda + 1/U)};$$

$$\theta = \frac{\phi_0(1 + \Lambda) \exp(-\xi/\Lambda)]}{U(1 + 1/\Lambda + 1/U)} \tag{8}$$

At the ignition front $\xi = 0$, the solids are at the ignition temperature $T_p(0) = T_{ig}$ and $\theta = 1$; this gives the solution for the velocity of the ignition front in dimensionless form as

$$U = \phi_0\Lambda - \Lambda/(1 + \Lambda) \tag{9}$$

which in dimensional form is

$$w_{ig} = \frac{1}{C'''} \left(\frac{q''_0}{T_{ig} - T_\infty} - \frac{\dot{C}''_g}{1 + \alpha\dot{C}''_g/(hS''')} \right) \tag{10}$$

The radiative flux depends on the effective temperature of the flame zone T_f, $q''_0 = K\sigma T_f^4$, where K (<1) is the effective radiation coefficient. T_f depends on the stoichiometry, the calorific value of the fuel, etc.

Equation 10 predicts that the flame will propagate, when the effective radiation temperature exceeds the critical value

$$T_f > \left(\frac{\dot{C}''_g(T_{ig} - T_\infty)}{K\sigma(1 + 1/\Lambda)} \right)^{1/4} \tag{11}$$

In this treatment, it has been assumed that the temperature of the gas far from the ignition

plane is the same as that of the solid. If the air is preheated, the velocity of the ignition front will accelerate. It is possible to estimate this effect by using formulae for transient temperatures in packed beds [37]. The effect of drying can also be estimated [38]. In the limiting case, if heat recovery by the gas flow is assumed negligible ($\Lambda \to 0$), we obtain $w_{ig} = q''_0/[C'''(T_{ig} - T_\infty)]$.

Effect of Moisture

Wooden fuels usually contain moisture. The propagation of the ignition front is described by the quasi-steady energy balance

$$\frac{\mathrm{d}(q'' - \dot{C}''T_g)}{\mathrm{d}x} = w_{ig}\frac{\mathrm{d}Q'''}{\mathrm{d}x} \tag{12}$$

where $q'' - \dot{C}''T_g$ describes the heat flux and Q''' denotes the energy per unit volume required to heat the solids and evaporate the water, so

$$Q''' = (1 - \epsilon)\rho_p[c_pT_p + u(l_{vap} + c_wT_p)] \tag{13}$$

Integration of Eq. 12 gives the ignition velocity in a fuel bed of thin, moist wooden chips as

$$w_{ig} = [q''_0 - \eta_g\dot{C}''_g(T_{ig} - T_\infty) - \eta_{vap}\dot{C}''_{vap}(T_{ig} - T_{vap})]/Q'''_{ig} \tag{14}$$

where

$$Q'''_{ig} = (1 - \epsilon)\rho_p(c_p(T_{ig} - T_\infty) + u_\infty[l_{vap} + c_w(T_{vap} - T_\infty)]) \tag{15}$$

The coefficients $\eta_g = (T_{g,ig} - T_\infty)/(T_{ig} - T_\infty) < 1$ and $\eta_{vap} = (T_{g,ig} - T_{vap})/(T_{ig} - T_{vap})$ account for the fact that the gas temperature is lower than the ignition temperature of the solids at the ignition plane. η_{vap} can be related to η_g by $\eta_{vap} = [T_\infty - T_{vap} + \eta_g(T_{ig} - T_\infty)]/(T_{ig} - T_{vap})$. In the case $u_\infty = 0$, $\eta_g = \Lambda/(1 + \Lambda)$, which can be seen by comparing Eqs. 14 and 10. Equation 14 predicts that ignition will take place provided that $T_f > \{[\eta_g\dot{C}''_g(T_{ig} - T_\infty) + \eta_{vap}\dot{C}''_{vap}(T_{ig} - T_{vap})]/\sigma K\}^{1/4}$. For fuels other than *a* (see "Experimental" section) the particles are not thin. Then the particle's temperature is nonuniform, the interior of the particle may still be wet, and only the outer surface of the particle is at the ignition temperature at the time of ignition. In this case the energy required to heat the particle to the ignition state is less than Q_{ig} (see Eq. 15).

Effect of Particle Size

Here it is assumed that the wooden chips are plates (so $\Gamma = 0$). $q'' = q''_0 \exp(\alpha w_{ig}t)$, where the time t is defined in the range $t = -\infty \ldots 0$ and $t = 0$ corresponds to the instant when the surface reaches the ignition temperature. A simplified problem is studied in order to obtain an analytical solution able to illustrate the effect of different parameters, such as particle size. The heat is assumed to be absorbed symmetrically on the surfaces of the plate (or perfect insulation is assumed on the plane of symmetry). In practice, however, the fuel has a size distribution and wooden chips may have thin sharp edges, which are ignited more easily. Also the radiative flux to the solids is not symmetrical in practice; this leads to numerical solutions of three-dimensional heat conduction problems for a specific configuration of the solids in the bed. Here the fuel is assumed to consist of plates of a constant thickness. The analysis could be extended to cylinders or spheres. Heat transfer to the particles, when convection is neglected, can be described by Fourier's equation:

$$\frac{1}{a_p}\frac{\partial T_p}{\partial t} = \frac{\partial^2 T_p}{\partial r^2} \tag{16}$$

with the initial, final, and boundary conditions

$$T_p(-\infty, r) = T_\infty,$$

$$T_p(0, R) = T_{ig},\ \lambda_p\left(\frac{\partial T_p}{\partial r}\right)_{r=R} = (\alpha q''_0/S''')\exp(\alpha w_{ig}t),$$

$$\left(\frac{\partial T_p}{\partial r}\right)_{r=R} = 0 \tag{17}$$

Equation 16 with the boundary conditions of Eq. 17, can be solved by applying the finite Fourier cosine transform [39]

$$\tilde{f}(n) = \int_0^R f(r)\,\cos(n\pi r/R)\,\mathrm{d}r \tag{18}$$

Using the transform $\tilde{f}(n)$ Eq. 16 becomes

$$\frac{1}{a_p}\frac{\mathrm{d}\tilde{T}_p}{\mathrm{d}t} = \frac{\alpha q''_0}{S'''\lambda}\cos(n\pi)\,\exp(\alpha w_{ig} t) - (n\pi/R)^2 \tilde{T}_p \tag{19}$$

The solution for the transformed transient temperature of the particles becomes

$$\tilde{\theta} = \frac{(-1)^n a_p \alpha q''_0/[S'''\lambda(T_{ig} - T_\infty)]}{\alpha w_{ig} + a_p(n\pi/R)^2}\exp(\alpha w_{ig} t) \tag{20}$$

The temperature distribution is found by applying the inverse transform [39]

$$f(r) = \frac{1}{R}\tilde{f}(n=0) + \frac{2}{R}\sum_{n=1}^{\infty}\tilde{f}(n)\,\cos(n\pi r/R) \tag{21}$$

giving

$$\theta = \frac{a_p \alpha q''_0}{RS'''\lambda_p(T_{ig} - T_\infty)}\left(\frac{1}{\alpha w_{ig}} + 2\sum_{n=1}^{\infty}\frac{(-1)^n\cos(n\pi r/R)}{\alpha w_{ig} + a_p(n\pi/R)^2}\right)\exp(\alpha w_{ig} t)$$

$$= \frac{\alpha q''_0}{RS'''\lambda_p(T_{ig} - T_\infty)\sqrt{\alpha w_{ig}/a_p}}\frac{\cosh(r\sqrt{\alpha w_{ig}/a_p})}{\sinh(R\sqrt{\alpha w_{ig}/a_p})}\exp(\alpha w_{ig} t) \tag{22}$$

At ignition, $t = 0$ and $\theta = 1$, and we obtain the relationship

$$\sqrt{U_*}\,\tanh(\sqrt{U_*}) = \Phi \tag{23}$$

between the dimensionless ignition velocity $U_* = R^2\alpha w/a_p$ and the dimensionless heat flux $\Phi = \alpha q''_0 R/[S'''\lambda_p(T_{ig} - T_\infty)]$. Equation 23 gives the dependence $U_* = F_1(\Phi)$ or $w_{ig} = a_p F_1(\Phi)/(R^2\alpha)$. For small values of $\Phi(\to 0)$, $U_* \to \Phi$, i.e., $w_{ig} \approx q''_0/[\rho_p c_p S''' R(T_{ig} - T_\infty)]$, which does not depend on R if the porosity of the bed remains constant, since $S''' = (1 + \Gamma)(1 - \epsilon)/R$. This is the same result as given by Eq. 10 for the case $\Lambda = 0$. For large values of Φ $(\to\infty)$, $U_* \to \Phi^2$, i.e., $w_{ig} \approx \alpha q''^2_0/[\rho_p c_p \lambda_p S'''^2(T_{ig} - T_\infty)^2]$. In this case w_{ig} is directly proportional to R, if $\alpha \propto S''' \propto 1/R$. Both dimensionless quantities depend on the particle's size. The effect of this size can be seen more clearly by using the dimensionless velocity $U_*/\Phi = F_2(\Phi)$, which does not depend on R, if the porosity is constant. Then we obtain the relation $w_{ig} = q''_0 F_2(\Phi)/[(1 + \Gamma)C'''(T_{ig} - T_\infty)]$.

Let us finally consider the case of parallel plates, with the distance between the plates, R_g, kept constant, but the thickness, R, of the plates changes and radiation through the gas $q'_g = q''_0(R + R_g)$ is assumed to be independent of R. In this case, α and $U_*/\Phi^2 = F_3(\Phi)$ do not depend on R and we obtain $w_{ig} = \alpha(q''_0/S''')^2 F_3(\Phi)/[\lambda_p\rho_p c_p(T_{ig} - T_\infty)^2] = \alpha q'^2_g F_3(\Phi)/[\lambda_p\rho_p c_p(T_{ig} - T_\infty)^2]$. The functions $F_1(\Phi)$, $F_2(\Phi)$ and $F_3(\Phi)$ are presented in Fig. 3.

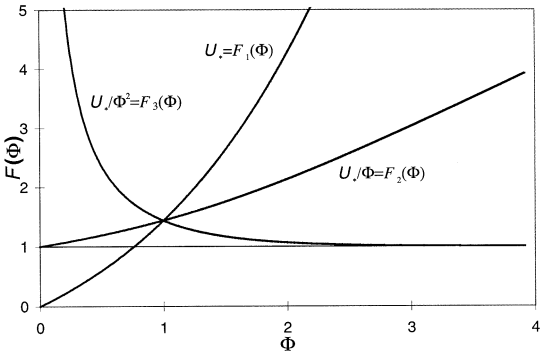

Fig. 3. The functions $F_1(\Phi)$, $F_2(\Phi)$, and $F_3(\Phi)$.

Thick Moist Solids

As a limiting case, very large particles are considered. Then the solids can be approximated as semi-infinite, since only a thin layer has been dried at the time of ignition. The drying of the surface layer of the solid can be described by the simplified equation

$$q'' = \frac{\lambda_p}{\delta}(T_s - T_{vap}) = \rho_p u_\infty l_{vap}\frac{\mathrm{d}\delta}{\mathrm{d}t} \tag{24}$$

when the temperature distribution in the dry surface layer (thickness δ) is approximated as linear. The first term, q'', is the radiation ab-

sorbed at the surface. It is also that conducted through the dry surface layer, as accounted for by the second term in Eq. 24. Finally it is the energy consumed in vaporization, as accounted for by the last term. The energy of vaporization is assumed to be much greater than that for heating the material and the liquid water, but the accuracy can be improved if this sensible heat is accounted for by using an effective heat of vaporization. Eq. 24 can be solved to give

$$w_{ig} = \alpha(q''_0/S''')^2/[\lambda_p \rho_p u_\infty l_{vap}(T_{ig} - T_{vap})] \quad (25)$$

Energy is consumed also in heating the combustion air; here it can be approximately taken into account by using an effective heat flux $q''_0 - \eta_g \dot{C}''_g(T_{ig} - T_\infty) - \eta_{vap}\dot{C}''_{vap}(T_{ig} - T_{vap})$ instead of q''_0.

Adiabatic Temperature of the Flame from the Volatiles

Steam from drying and volatiles are released to the gas flow. The volatiles are assumed to be $CH_{2.26}O_{0.99}$ and also to react by $CH_{2.26}O_{0.99} + AO_2 \rightarrow B_1CO + B_2CO_2 + B_3H_2O + B_4CH_4$. This is for a typical elemental composition of wood, if the char is assumed to consist of carbon and its yield is 18 wt %. The coefficient A and the heat of decomposition ΔH_{vol} are defined by the stoichiometry; A depends on the primary air mass flux $\dot{m}''_g$ and the mass flux of the volatiles generated. The mass flux of dry fuel to the moving flame zone is related to the velocity of the ignition front $\dot{m}''_p = (1 - \epsilon)\rho_p w_{ig}$ and the mass flux of the volatiles is $\dot{m}''_{vol} = \nu(1 - \epsilon)\rho_p w_{ig}$. The coefficient $A = (Y_{O2}\dot{m}''_{g0}/M_{O2})/(\dot{m}''_{vol}/M_{vol})$. The values of B are readily calculated from the balances for C, H, and O, when A is known. The flux of water vapor generated due to moisture is $\dot{m}''_{vap} = (1 - \epsilon)u\rho_p w_{ig}$.

The adiabatic temperature of the flame from burning the volatiles can be estimated from a simple heat balance on the moving flame zone, if it is assumed that the gases leave the zone at that temperature. The heat balance is

$$\sum_{i=1}^{g} q'' = 0 \quad (26)$$

where the terms $q''_1 = \nu\dot{m}''_p\Delta H_{vol}$; $q''_2 = -\nu\dot{m}''_p l_{vol}$; $q''_3 = -u_\infty\dot{m}''_p l_{vap}$; $q''_4 = c_w u_\infty \dot{m}''_p(T_\infty - T_{vap})$; $q''_5 = c_p\dot{m}''_p\ (T_\infty - T_{vol})$; $q''_6 = \dot{C}''_g(T_\infty - T_a)$; $q''_7 = c_{vol}\nu\dot{m}''_p\ (T_{vol} - T_a)$; $q''_8 = c_{vap}u_\infty\dot{m}''_p(T_{vap} - T_a)$; and $q''_9 = c_c\kappa(1 - \nu)\dot{m}''_p\ (T_{vol} - T_a)$ are the energies associated, respectively, with combustion of the volatiles, the pyrolysis reactions, the evaporation of water, heating of water to the temperature for evaporation, heating of particles to the devolatilization temperature, heating of combustion air to the reaction temperature, heating of volatiles to the reaction temperature, heating of water vapor to the reaction temperature, and the heating of char close to reaction temperature. Due to a time lag, the char does not reach the gas temperature, which is accounted for by assuming a value of 0.9 for the coefficient κ. Equation 26 gives

$$T_a = \frac{\sum_{i=1}^{5} q''_i + \dot{C}''_g T_0 + \dot{m}''_p\{[c_{vol}\nu + c_c\kappa(1 - \nu)]T_{vol} + c_{vap}u_\infty T_{vap}\}}{\dot{C}''_g + \dot{m}''_p[(c_{vol}\nu + c_c\kappa(1 - \nu) + c_{vap}u_\infty]} \quad (27)$$

At low flow rates of air, the temperature of the reaction zone can be assumed to be close to the adiabatic flame temperature (so $T_f \approx T_a$), when the particles are small. Then the effects of air flow rate (reaction stoichiometry) and moisture on the temperature are adequately described by Eq. 27. When the particles are large, volatiles are released in a thicker zone and the difference between the effective radiating flame temperature T_f and the adiabatic flame temperature T_a will be greater. The thickness of the zone, where simultaneous drying and pyrolysis take place, can be calculated from the relationship $L_d = t_d w_{ig}$, where t_d is the drying and pyrolysis time of the particles as estimated by a model presented earlier [40].

DISCUSSION

The size, shape, and orientation of a particle affect the local turbulence, the mixing of fuel-volatile with oxygen, and also combustion in the

bed, all of which are important factors affecting ignition. The particles used in the experiments do not have a specific shape and size, since they are fuels used in practice. Consequently, times for ignition and ignition temperatures in a bed of fuel vary from case to case due to the random size, shape, and orientation of the particles in the bed. However, it is important to get some quantitative approximation for the velocity of the ignition front. Here we suggest the use of Eq. 14. The time needed to heat a particle to the ignition temperature is directly proportional to the particle's density and specific heat by theory. Thus the velocity of the ignition front is inversely proportional to the bulk density of the dry mixture $\rho_b = (1 - \epsilon)\rho_p$ and specific heat of wood, which are included in Eq. 14. The fuel's properties (bed density, moisture, and specific heat) can be measured. More difficult is the determination of the parameters related to radiation and convection and also modeling of the particle size effects. These effects are lumped into an experimental coefficient K and the maximum temperature T_{max}, which is assumed to correspond to the effective radiation temperature T_f. The coefficient K was evaluated from Eq. 14 by using measured values of w_{ig} and T_{max}. Values of $c_p = 2000$ J kg^{-1}, $T_\infty = 293$ K, $T_{ig} = 650$ K, and $\eta_g = \eta_{vol} = 0$ were used in these calculations.

The flux of volatiles at the surface of a particle depends on its size, so that $\dot{m}''_{vol} \sim R^{1-n}$, if the devolatilization time is $\sim R^n$. A simple analysis shows that the distance δ from the ignition front (see Fig. 1), where the gas mixture reaches the stoichiometric fuel/oxygen ratio, depends on the flow rate of air, $\dot{m}''_g$, and the size of particles, R, by $\delta \sim \dot{m}''_g R^n$, since $S''' \sim 1/R$. If we roughly assume that the stoichiometric condition corresponds to the maximum flame temperature T_f and that radiation also decays exponentially between the locations of maximum temperature and ignition, we obtain a simple relationship $K = K_f \exp(-\alpha\delta) \approx K_f - const. \times \dot{m}''_g R^{0.5}$, since $\alpha \sim 1/R$ and $n = 1.5$ [42, 43]. K_f is a constant. This approximately linear relationship with respect to $\dot{m}''_g$ is seen in Fig. 4. It also predicts that K is higher for small particles, which is seen in Fig. 4, when comparing fuels a, b, and c. The largest c particles are practically dry and the release of volatiles becomes faster than with the other fuels, making δ smaller; this is probably the reason for the relatively high values of K for this fuel. The available data are too scarce to obtain a single expression for K accounting for the effects of a particle's size and moisture content. Experiments with particles of different sizes but equal shape are needed to develop this.

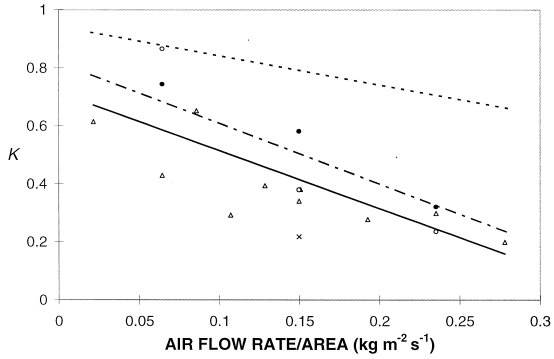

Fig. 4. Calculated effective radiation coefficient K based on the measured ignition velocity and maximum temperature in the bed. Fuel b (moistures are 10.8 △, 11.4 ▲, 18.8 ○, 27.1 ×, and 33.4 ● % in wet basis), solid trendline; fuel a dashed trendline; fuel c dotted trendline.

The following correlations for T_f and K can be used in Eq. 14 in units of K and kg m^{-2} s^{-1}, when fuel moisture (wet basis) is below 30%. For fuel a $T_f = 997.8 + 1415\,\dot{m}''_g - 1646\,\dot{m}''^2_g$ and for other fuels $T_f = 903.2 + 5547\,\dot{m}''_g - 11{,}626\,\dot{m}''^2_g$. The best lines for the radiation coefficients are for fuel a: $K = 0.943$–$1.008\,\dot{m}''_g$, for fuel b: $K = 0.714$–$2.002\,\dot{m}''_g$, and for fuel c: $K = 0.819$–$2.100\,\dot{m}''_g$. At $\dot{m}''_g = 0.15$ kg m^{-2} s^{-1} the values of K obtained from the trendline were 0.79, 0.41, 0.50 for fuels a, b, and c, respectively. For fuel d the values $K = 0.30$, 0.28, and 0.25 were obtained for particle sizes 7–13, 13, and 30 mm. For fuel e the values $K = 0.53$ and 0.30 were obtained for small and large size fractions, respectively. In addition, one experiment with wooden pellets gave $K = 0.24$. Thus, there are rather large differences between the fuels, which could be due to differences in a fuel's properties other than bed density or moisture, such as the kinetics of pyrolysis, the products of pyrolysis (including ignition temperature), and specific heat, for which a constant value of 2000 J kg^{-1} was assumed. In addition, differences in shape and size distributions and orientation of the particles affect K.

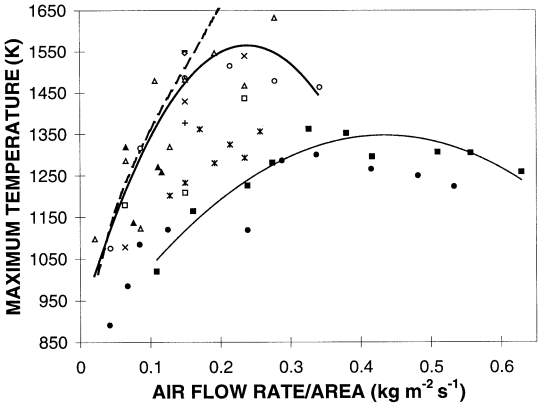

Fig. 5. Effect of flow rate of air on the maximum temperature measured by the middle thermocouple. Fuels (and moisture contents in wet basis) are *a* (8.9%, ■, trend line; 17.3% ●; 29.7% ▲), *b* (10.8% △; 11.4% +; 18.8% ×; −27.1%; □ 33.4%), *c* (○ 2.1%) and *d* (◇ 12.7%; 32.3–33.9% ***). The upper solid line is the best-fit second-order polynomial for points for fuels *b*, *c*, and *d* with moisture <30%. The dashed line is the calculated adiabatic temperature.

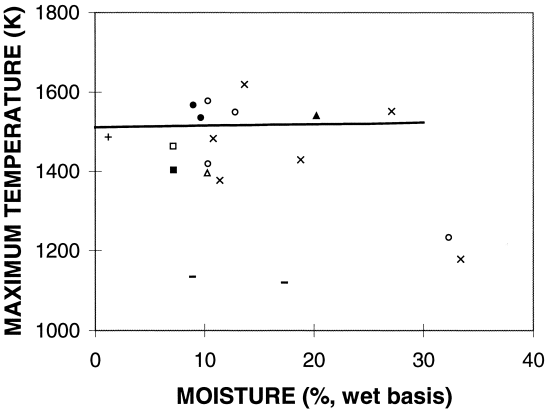

Fig. 6. Effect of fuel moisture on the maximum temperature measured by the middle thermocouple. Fuels are *a* (−), *b* (×), *c* (+), *d* (□ 7–13 mm, ○ 13 mm, ● 30 mm), *e* (△ small, ▲ large), and wood pellets (■). The line is the calculated adiabatic temperature. Air rate is 0.15 kg m^{-2} s^{-1}.

Figure 5 shows the effect of the flow rate of air on the measured maximum temperature inside the bed. The temperatures in a bed of the thin particles *a* are clearly lower than those of other fuels with larger particles. For larger alder particles, the maximum temperature in the bed was higher than for smaller ones. A similar trend was obtained for birch particles, if average values of the points for each size are used. The lower maximum temperatures of fuel consisting of smaller particles can partly be explained by the higher value of K (greater losses from the flame). Another reason might be a lower value of κ for larger nonisothermal particles. Figure 6 shows that moisture seems to have no influence on the maximum temperature, when the moisture content of the fuel is below ~30% (wet basis). The calculated adiabatic temperature also predicts this. Increase in the moisture content decreases the velocity of the reaction front, changing the conditions more rich with oxygen, since the rate of devolatilization decreases. The net result is that the temperature remains quite constant, in spite of the increasing amount of energy consumed in vaporization.

The adiabatic temperatures for fuel *b* with moisture 10.8% shown in Figs. 4 and 5 were calculated iteratively from Eqs. 14 and 27. The velocity of the ignition front was estimated by Eq. 14 using the correlation presented above for K and assuming $T_f = T_a$. Figure 4 shows that, when the air rate is small, the adiabatic temperature is close to the best-fit second-order polynomial. At higher flow rates of air, the calculated adiabatic temperature becomes higher than the measured maximum temperature, which is believed to be due to the endothermic gasification reaction ($C–CO_2$ and $C–H_2O$), which becomes important at high temperatures, decreasing the temperature, but was not included in the calculation of T_a.

The measured velocities of the ignition front presented in the literature for counterflow systems are summarized in Fig. 7. The velocity reaches a maximum at a specific flow rate of air for fuel *a* (thin wood chips) as shown in Fig. 8. It is also seen that the ignition front moves only for a specific range of flow rates of the primary air; otherwise combustion is extinguished. The range of flow rates for a moving front becomes narrower with increasing moisture content, so the ignition front no longer propagates above a specific moisture level. The model predicts the effects of both the flow rate of air and moisture, but not the limits of sustaining combustion. Similar trends are seen in Fig. 9 for fuel *b* with medium size particles; here the flame speed depends on the flow rate of air to some extent at moisture contents of 10.8 and 18.8 wt % (wet basis), but is rather constant at a moisture

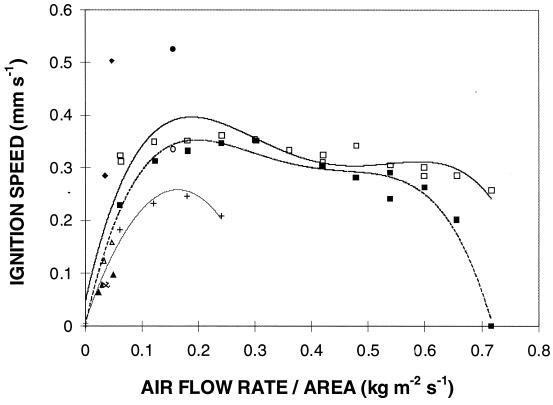

Fig. 7. Summary of literature values of the velocity of the front in beds of wooden particles: Birch 11% [30] (●), birch 38% [30] (○), willow 28% [28] (△), willow 40% [28] (▲), softwood 40% [28] (×), softwood 13% [28] (◆), wood 30 mm, 10% [25] (□, solid trendline), wood 10 mm, 10% [25] (■, dashed trendline), wood 10 mm, 30% [25] (+, thin solid trendline) on a wet basis. The ignition velocities for the results of Gort [25] have been calculated by assuming a dry bed density of 200 kg m^{-3}.

content of 34.4 wt %. For the largest, almost dry, particles *c*, Fig. 9 shows no such maximum. In fact, the ignition speed slightly increases with decreasing flow rates of air. However, it is clear that if the flow rate is further decreased, the ignition speed must decrease, since in the limiting situation of zero flow rate, the speed must be zero. From a pollution point of view it is more favorable to choose a flow rate for air below that giving the maximum ignition speed,

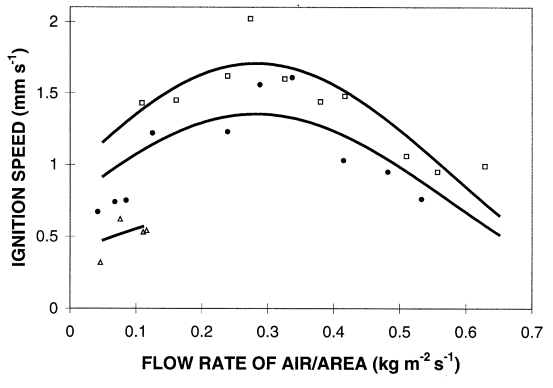

Fig. 8. Measured and calculated velocity of the ignition front as a function of the flux of primary air in a bed of wood particles (fuel *a*) with different moistures 8.9 (□), 17.3 (●), and 29.7% (△) on a wet basis. Solid lines are calculated by Eq. 14, $\eta = 0$, $\rho_b = 58$ (8.9), 57 (17.3), and 76 kg m^{-3} (29.7%).

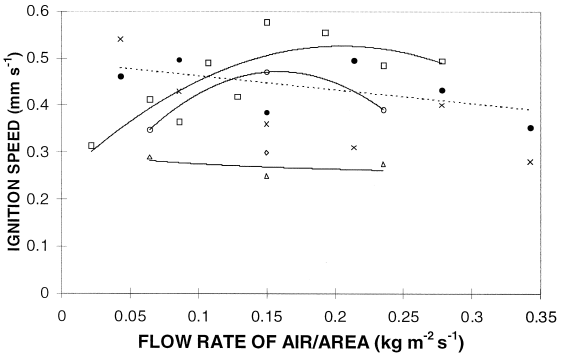

Fig. 9. Measured velocity of the ignition front as a function of the flux of primary air in a bed of wooden particles. Open symbols are for fuel *b* (spruce, 5–20 mm, moistures are 10.8 □, 18.8 ○, 27.1 ◇, and 33.4% △ on a wet basis, solid trendlines) and filled ones for fuel *c* (mixture of spruce and pine, 31 mm, 2.1% ● on a wet basis, dashed trendline; × based on visual observations).

since fuel-rich conditions are usually more favorable, when considering NO formation [41]. Also fewer particles are entrained from the grate. It is not possible to increase significantly the combustion intensity from the devolatilization zone of the grate beyond the air rate giving the maximum ignition velocity, since the mass flux of volatiles released from the bed is directly proportional to the velocity of the ignition front. However, the rates of char combustion and gasification above the flame zone increase with the flow rate of air.

The flame temperature depends on the local ratio of [fuel]/[O_2] and reaches a maximum at a specific flow rate of air. After that, increasing the flow rate of air dilutes the gas in the flame, so the temperature falls. The rate of pyrolysis depends on the particle size and the pyrolysis time is usually represented by a power law $t \sim d^n$, where $n = 1.5$ [42, 43]. For small particles, the rate of devolatilization is faster and more volatiles are available in the flame zone. When the flow rate of the air and the temperature are constant, the ratio of fuel mass to oxidizer at the start of the flame zone is proportional to $1/d^{1.5}$. Then the maximum velocity of the ignition front is reached for small particles (Fig. 8) with a higher flow rate of air than for larger ones (Fig. 9) with moisture contents less than ~20%. If the particles are large, the rate of generation of volatiles in the flame zone is not so intense. Then, increasing the flow rate will lead to a

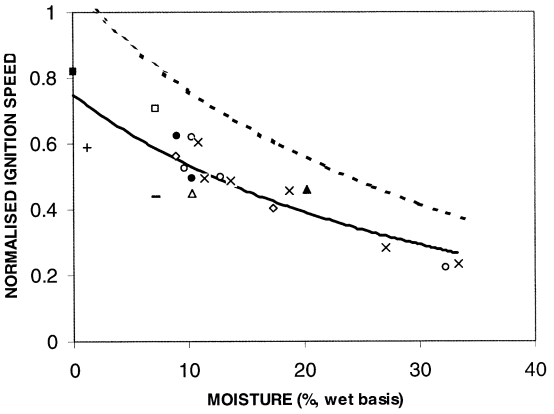

Fig. 10. Measured and calculated effect of fuel moisture content on the normalized ignition velocity. Mass flux of air is 0.150 kg m^{-2} s^{-1}. Measurements: fuels and average dry bed densities (ρ_b) are *a* (◇, 54 kg m^{-3}), *b* (×, 149 kg^{-3}), *c* (+, 230 kg m^{-3}), *d* (□, 7–13 mm, 196 kg m^{-3}; ○, 13 mm, 210 kg m^{-3}; ●, 30 mm, 216 kg m^{-3}), *e* (△, small, 140 kg m^{-3}; ▲, large, 141 kg m^{-3}) and wood pellets (−, 8 mm, 612 kg m^{-3}). Calculated results: solid line is Eq. 14 with $\eta = 0$; point ■ is Eq. 23 with $R = 0.01$ m; dashed line is Eq. 25 with effective heat of vaporization [$= l_{vap} + c_p(T_{ig} - T_\infty)/u$]. In the calculations $K = 0.3$, $T_f = 1473$ K, $c_p = 2000$ J kg K, $S''' = 150$ m^{-1}, $\alpha = 37.5$ m^{-1}, $\rho_p = 500$ kg m^{-3}, and $\lambda_p = 0.14$ Wm^{-1} K^{-1}.

decrease in the flame temperature, due to dilution with excess air, resulting in a decrease in the velocity of the ignition front after the optimal stoichiometric condition. This takes place at a lower flow rate of air than for smaller particles, as seen from Fig. 9 by comparing fuels *b* (medium size particles) and *c* (large particles). If flue gas recirculation is applied, the oxygen content is lower and more oxidizing gas is required for the same stoichiometric conditions; this decreases the flame temperature and the propagation rate.

The maximum ignition speed for the thin particles (Fig. 8) is greater than that for the larger ones (Fig. 9), but this is mainly due to the difference in bulk density of the bed, which was small for thin particles. Equation 23 (and also Eq. 25) predicts that the velocity of the ignition front increases with a particle's size provided that K is constant. However, measurements and the simple analysis indicate K decreasing with increasing size; this has the opposite effect on the velocity. Figure 10 shows no clear experimental effect of the size of a particle on ignition velocity. The ignition mass fluxes, defined as $\dot{m}''_{ig} = \rho_b w_{ig}$, are of equal magnitude for a wide range of dry bed densities (56 to 612 kg m^{-3}) as seen in Fig. 10, where the ignition velocities have been normalized to the reference dry density $\rho_{b,ref} = 150$ kg m^{-3} by multiplying the measured ignition velocity with $\rho_b/\rho_{b,ref}$. Equation 23 (and also Eq. 25) predicts that the ignition velocity is lower for materials with a higher thermal conductivity, especially when the size of the particles is large. The normalized velocity is clearly lower for the dense wooden pellets with a high thermal conductivity (caused by the greater density).

An increasing moisture content of the wood particles decreases the flame speed in two ways: the temperature of the ignited region decreases due to dilution, and the energy needed to heat (and dry) the particles to the ignition temperature increases. Figure 10 shows that the calculations using Eq. 14 predict the effect of moisture content quite well. The treatment of the solids as thermally thick (Eq. 25) gives the same trend, but at a higher level; the thickness of the dried layer at the moment of ignition is $\delta_{p,ig} = S'''\lambda_p(T_{ig} - T_{vap})/(\alpha q''_0) = 1.7$ mm.

In practical grates, the movement of parts of a grate relative to the others or vibrations can increase the velocity of propagation of the ignition front. The direction of the combustion air can also be such that it entrains hot combusting gases to heat the nonignited fuel convectively, thereby increasing the speed of the front.

CONCLUSIONS

Ignition in beds of wood particles has been studied for the incoming air and propagating ignition wave in counterflow. Modeling the effects of the flow rate of air, the moisture content of the fuel, particle size, and properties of wood (density, specific heat, thermal conductivity) is discussed and used for interpreting the experimental measurements. A sustained ignition wave is obtained over a specific range of flow rates of air, depending on the moisture content of the fuel. At very low flow rates of air, the flame temperature remains too low, due to a lack of oxygen, so extinction takes place. As the flow rate of air is increased, the conditions close to the ignition front change from fuel-rich to

oxygen-rich. Then the gases are diluted with excess air, so temperatures decrease, resulting in extinction, when a specific flow rate of air is reached. Increasing this flow rate also moves the region of the maximum temperature farther away from the ignition front, decreasing the radiation from the hot combusting zone.

Several experiments studied the effects of the flow rate of air, the moisture content of the fuel, the particle size, the density of the bed, and the type of wood. Moisture was found to significantly lower the speed of the ignition front. However, moisture did not have any noticeable effect on the maximum temperature in the bed, when the moisture content (wet basis) was less than 30 wt %. No effect of particle size on the ignition front's speed was found, but increasing the particle size increased the maximum temperature in the bed to some extent. The velocity of the front was found to be inversely proportional to the density of the fuel bed and the specific heat of wood. Also the velocity of the ignition wave and the maximum temperature in the fuel bed were found to reach maximum values at specific flow rates of air. Correlations for the maximum bed temperature and the effective radiation coefficient in the bed are presented. The effect of the principal factors, such as the flow rate of air, moisture content, and the density of fuel on the ignition velocity can all be explained by modeling.

Support from the Commission of the European Community through contract JOR3-CT96-0059 (JS & RT) and from the Technology Developing Centre of Finland (TEKES), contract 40760 (MH) is acknowledged.

REFERENCES

1. Hottel, H. C., Williams, G. C., and Steward, F. R., *Tenth Symposium (International) on Combustion*, The Combustion Institute, Pittsburgh, 1965, p. 997.
2. Fang, J., and Steward, F., *Combust. Flame* 13:392 (1969).
3. Berland, A. L., *Combust. Flame* 14:123 (1970).
4. Steward, F. R., *Combust. Sci. Technol*. 4:177 (1971).
5. Berland, A. L., Rothermel, R. C., and Frandsen, W., *13th Symposium (International) on Combustion*, The Combustion Institute, Pittsburgh, 1971, p. 927.
6. Rothermel, R. C. (1972). *A Mathematical Model for Predicting Fire Spread in Wildland Fuels*, USDA Forest Service, Research Paper INT-115.
7. Pagni, P. J., and Peterson, T. G., *Fourteenth Symposium (International) on Combustion*, The Combustion Institute, Pittsburgh, 1972, p. 1099.
8. Carrier, G. F., Fendell, F. E., and Wolff, M. F., *Combust. Sci. Technol*. 75:31 (1991).
9. Dunningham, A. C., and Grumell, E. S., *J. Inst. Fuel*, 11:129 (1937), p. 129.
10. Crumell, E. S., and Dunningham, A. C., *J. Inst. Fuel,* 12:87, (1938).
11. Mayers, M. A., and Landau, H. G., *Ind. Eng. Chem*. 32:563 (1940).
12. Carman, E. P., and Reid, W. T., *Trans. ASME* 67:425 (1945).
13. Graf, E., Carman, E., and Corey, R., *Combustion* 67:59 (1954).
14. Orning, A. A., Pfeiffer, J. J., Harold, W. C., and Shultz, J. F. (1958). *51st Annual Meeting of APCA*, Philadelphia, paper 58-12.
15. Weintraub, M., Orning, A. A., and Schwartz, C. H. (1967). U.S. Department of the Interior, Bureau of Mines, RI 6908.
16. Stumbar, J. P., Kuwata, M., Kuo, T., and Essenhigh, R. H., *Proc. 4th Nat. Incin. Conf*., ASME, New York, 1970, p. 288.
17. Rogers, J. E. L., Sarofim, A. F., and Howard, J. B., *Proc. 5th Nat. Incin. Conf*. ASME New York, 1972, p. 135.
18. Rogers, J. E., Sarofim, A. F., Howard, J. B., Williams, G. C., and Fine, D. H., *Fifteenth Symposium (International) on Combustion*, The Combustion Institute, Pittsburgh, 1975, p. 1137.
19. Rogers, J. (1973). Ph.D. thesis, Massachusetts Institute of Technology.
20. Ruimin, J., Hesheng, Z., and Dezhen, C., *3rd Asian-Pacific International Symposium on Combustion and Energy Utilization*, Hong Kong, 1995, p. 84.
21. Cozzani, V., Nicolella, C., Rovatti, M., and Tognotti, L., *Ind. Eng. Chem. Res*. 35:90 (1996).
22. Ford, N. W., Cooke, M. J., and Sage, P. W., *Fuel Proc. Technol*. 36:55 (1993).
23. Drew, D. A., *Combust. Sci. Technol*. 47:139 (1986).
24. Zhou, X., Torero, J. L., Goudeau, J. C., and Bregeon, B., *Combust. Sci. Technol*. 110–111:123 (1995).
25. Gort, R. (1995). Ph.D. thesis, University of Twente.
26. Gort, R., Valk, M., and Brem, G., *3rd Asian-Pacific Symposium on Combustion and Energy Utilization*, Hong Kong 1995, p. 312.
27. Stubington, J., and Fenton, H., *Combust. Sci. Technol*. 37:285 (1984).
28. Larfeldt, J., and Berge, N., *Biomass for Energy and Industry, 10th European Conference and Technology Exhibition*, 1998, p. 1486.
29. Aho, M., *J. Anal. Appl. Pyrol*. 11:149 (1987).
30. Aho, M. (1987). Technical Research Centre of Finland, Research Reports 465, Espoo.
31. Fatehi, M., and Kaviany, M., *Int. J. Heat Mass Transf*. 40:2607 (1997).
32. Ford, N., Cooke, M. J., and Pettit, M. D., *J. Inst. Energy* 65:137 (1992).
33. Saastamoinen, J., Huttunen, M., and Kjäldman, L., in *Computational Fluid Dynamics '98*, Vol. 2 (K. D.

Papailiou, D. Tsahalis, J. Périaux, and D. Knötzer, Eds.), John Wiley, Chichester, 1998, p. 814.
34. Janssens, M., *Fire Mater*. 15:151 (1991).
35. Tzeng, L. S., Atreya, A., and Wichman, I. S., *Combust. Flame* 80:94 (1990).
36. Simms, D. L., and Law, M., *Combust. Flame* 11:377 (1967).
37. Riaz, M., *ASME J. Heat Transfer* 99:489 (1977).
38. Saastamoinen, J., and Impola, R., *Drying Technol*. 15:1919 (1997).
39. Churchill, R. V., *Operational Mathematics*, 3rd ed., McGraw-Hill Kogakusha, Ltd., Tokyo, 1972.
40. Saastamoinen, J., and Richard, J.-R., *Combust. Flame* 106:288 (1996).
41. Russel, S. H., and Roberts, J. E., *ASME J. Energy Resources Technol*. 107:285 (1985).
42. Ragland, K. W., and Weiss, C. A., *Energy* 4:341 (1979).
43. Stubinton, J. F., Huang, G., and Scaroni, A. W., *Fuel* 70:1105 (1991).

Received 21 June 1999; revised 6 March 2000; accepted 16 March 2000